Exciton spectra and anisotropic Zeeman effect in PbI_2 at high magnetic fields up to 40 T

Y. Nagamune,* S. Takeyama, and N. Miura
Institute for Solid State Physics, University of Tokyo, 7-22-1 Roppongi, Minato-ku, Tokyo 106, Japan
(Received 2 July 1990; revised manuscript received 21 December 1990)

Magnetoabsorption spectra of the band-edge excitons in PbI_2 thin single crystals were measured up to 40 T with a configuration of $\mathbf{E}\perp c\|\mathbf{B}$ or $\mathbf{E}\perp c\perp\mathbf{B}$. The anisotropic magnetic field dependence of the diamagnetic shift and the Zeeman effect were observed at high magnetic fields. With the configuration of $\mathbf{E}\perp c\|\mathbf{B}$, a linear Zeeman splitting of the Γ_3^- absorption line was observed. For the configuration of $\mathbf{E}\perp c\perp\mathbf{B}$, magnetic-field-induced absorption lines associated with the Γ_1^- and the Γ_2^- states were observed for π and σ polarizations, respectively. The anisotropic magnetic field dependence is discussed in terms of a cationic exciton model.

I. INTRODUCTION

PbI_2 is a typical layered semiconductor that shows large exciton structure below the band edge.[1] However, there has been a great deal of controversy concerning the assignment of the exciton lines as a Wannier series.[2–4] In a previous paper, it was shown that it is important to take exciton-phonon interaction into account to interpret the exciton structure with respect to the relative motion of electrons and holes.[5]

The valence and conduction bands of PbI_2 have a strong cationic character and their charge density is located around Pb^{2+} cationic ions as revealed by study of exciton spectra in $Pb_{1-x}Cd_xI_2$ alloys[6] and band calculations.[7] The existence of the three-exciton-line series *A*, *B*, and *C*, which arise from spin-orbit interaction, is well explained in terms of the semiempirical atomic model called the cationic exciton model.[7]

The Bohr radius of the ground-state exciton parallel to the layer plane is estimated as 1.9 nm.[5] This value is only about four times as large as the in-plane lattice constant. Although the exciton spectra in PbI_2 can be analyzed in terms of the Wannier-type exciton,[5] the above value of the Bohr radius is too small to characterize this exciton as an ideal Wannier-type exciton compared to the usual semiconductors. Based on a cationic exciton model taking account of electron-hole coupling,[8] it is expected that the band-edge exciton is split into three states, Γ_1^-, Γ_2^-, and Γ_3^- by the large electron-hole exchange interaction owing to such a small exciton radius as shown in Fig. 1, but the estimation of the energy positions of the three states are different according to different workers[8–10] and the Γ_1^- state has never been observed. Here, the characters of the three states are taken for the 2H-PbI_2 crystal symmetry of D_{3d}.[11] The Γ_3^- is an allowed transition for $\mathbf{E}\perp c$ and the Γ_2^- for $\mathbf{E}\|c$, where $\mathbf{E}$ is the electric-field vector of the incident light and c is the crystal axis perpendicular to the layer of PbI_2 crystal. The Γ_1^- exciton is a pure triplet state, which is optically forbidden.

If high magnetic fields are applied in this system with the configuration of $\mathbf{k}\|c$ and $\mathbf{E}\perp c\perp\mathbf{B}$, it is expected that a new absorption line arising from the Γ_1^- or Γ_2^- states is observed near the Γ_3^- exciton, where $\mathbf{k}$ is the wave vector of the incident light and $\mathbf{B}$ is the applied magnetic field. In this paper, we present the experimental results of high-field magnetoabsorption measurements up to 40 T with the configuration of $\mathbf{E}\perp c\|\mathbf{B}$ or $\mathbf{E}\perp c\perp\mathbf{B}$ and the observed anisotropic magnetic-field dependence of the exciton spectra. We demonstrate that the experimental results are qualitatively explained by the cationic exciton model.

II. EXPERIMENT

PbI_2 thin single-crystal samples with thicknesses of 50–100 nm were prepared by cleaving single-crystal ingots made by the traveling-zone technique.[12] Their polytype was found to be 2H with their exciton spectra compared to that of the reference sample estimated as 2H polytype by x-ray analysis.[12] For measurement of magnetoabsorption spectra, we employed a nondestructive-type

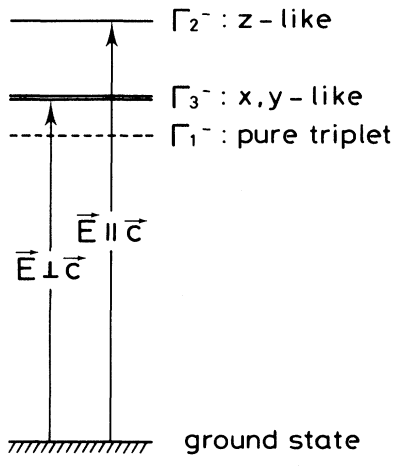

FIG. 1. Schematic illustration of the exciton energy levels in 2H-PbI_2 below the band edge.

pulse magnet and an optical-multichannel-analyzer (OMA) system.[13,14]

A pulsed magnetic field was generated by supplying a large current from a 112- or 200-kJ capacitor band into a coil made of Nb-Ti/Cu superconducting wire with a large mechanical strength. The magnet was cooled by liquid nitrogen to prevent the excess temperature rise by the current. The pulse width was about 10 ms and maximum field was about 40 T. An incident light was provided as a single pulse by a pulsed tungsten lamp or a xenon flash lamp. For the configuration of $\mathbf{E}\perp c\parallel\mathbf{B}$, the incident light was introduced by an optical fiber onto a PbI_2 sample on a quartz plate through a polarizer and a quarter-wavelength plate as shown in Fig. 2(a). The sample was placed at the center of the pulse magnet and cooled by liquid helium. Light coming through the sample is reflected by a prism and further transferred by another optical fiber to the entrance slit of the spectrometer. For $\mathbf{E}\perp c\perp\mathbf{B}$, the sample was put between two prisms together with a polarizer and a quartz plate as shown in Fig. 2(b). The image of the optical spectrum by the spectrometer is focused on a diode detector array. The OMA system is operated to a pulse mode by opening the gate in a duration time of 1 ms at the top of a pulsed magnetic field. The pulse width of the incident light was larger than the gate width of the OMA. The variation of magnetic field during the measurement was less than 3% at the top of the pulsed magnetic field. With the configuration of $\mathbf{E}\perp c\parallel\mathbf{B}$, left or right circularly polarized light, σ_+ or σ_-, was introduced onto the sample. For $\mathbf{E}\perp c\perp\mathbf{B}$, linearly polarized light, $\pi(\mathbf{E}\parallel\mathbf{B})$ or $\sigma(\mathbf{E}\perp\mathbf{B})$, was introduced. The wave vector of the incident light was parallel to the c axis ($\mathbf{k}\parallel c$). To increase the signal-to-noise ratio more than four data measured under the same condition were averaged by a computer. The spectral resolution determined by the slit width of the spectrometer was 0.43 nm for $\mathbf{E}\perp c\parallel\mathbf{B}$ and 0.13 nm for $\mathbf{E}\perp c\perp\mathbf{B}$. The resolution for the energy shift of the absorption lines is better than this value.

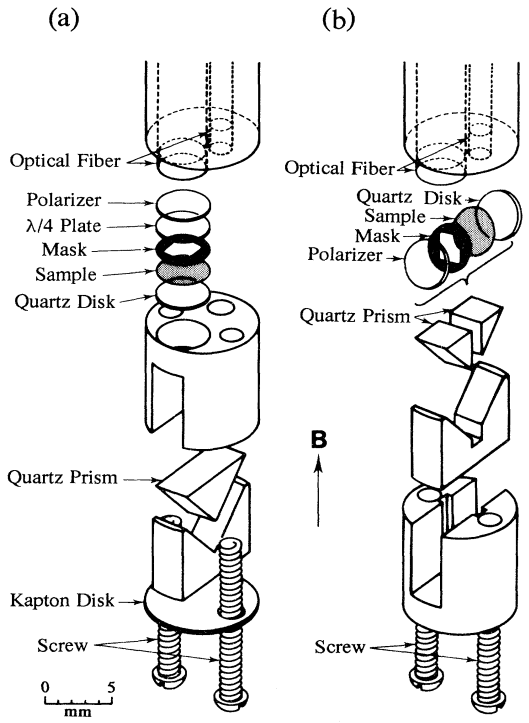

FIG. 2. Schematic illustration of the sample holder for (a) $\mathbf{E}\perp c\parallel\mathbf{B}$ and (b) $\mathbf{E}\perp c\perp\mathbf{B}$.

III. RESULTS AND DISCUSSION

An example of the experimental recordings for π and σ polarization of $\mathbf{E}\perp c\perp\mathbf{B}$ gyometry is shown in Figs 3(a) and 3(b), respectively, for various magnetic fields. As shown in these figures, besides the main absorption line addi-

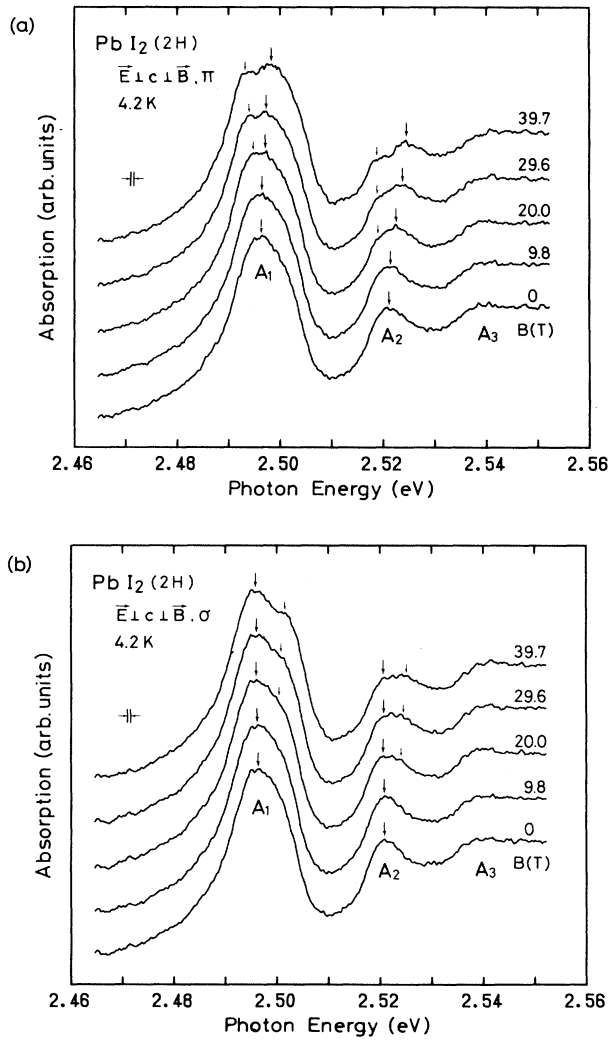

FIG. 3. Magnetoabsorption spectra 2H-PbI_2 at 4.2 K. (a) and (b) were obtained for π and σ polarization, respectively. Applied magnetic fields are indicated on the right-hand side of each spectrum. Large down arrows display main absorption lines, which correspond to the absorption lines at $\mathbf{B}=0$, and small down arrows indicate magnetic-field-induced new lines.

tional absorption lines indicated by small down arrows become discernible at high magnetic fields. Exciton absorption spectra for the four polarizations including the σ_+ and σ_- polarizations of $\mathbf{E}\perp c\|\mathbf{B}$ geometry are summarized in Fig. 4 for $\mathbf{B}=0$ T and $\mathbf{B}\cong 40$ T. Anisotropic magnetic-field dependence is clearly observed in the figures. The peak position of A_1 and A_2 exciton lines for $\mathbf{E}\perp c\|\mathbf{B}$ and $\mathbf{E}\perp c\perp\mathbf{B}$ are plotted as a function of applied magnetic field in Fig. 5. Energy splitting of the A_2 line is quite similar to that of the A_1 line as shown in Figs. 3–5. This shows that the A_2 line belongs to the same exciton series as that of the A_1 line as discussed in a previous paper,[5] namely the A_1 line is the $n=1$ state and the A_2 line is the $n=2$ state, where n denotes the main quantum number of the exciton.

From the energy difference between the ground-state absorption lines for σ_+ and σ_- polarizations, linear Zeeman splitting was obtained, and the effective g value was experimentally determined to be 0.89.[5] It is considered that the splitting for this configuration is that of the Γ_3^- state which is a twofold degenerate state according to the cationic exciton model. In order to examine how the cationic exciton model is appropriate for interpreting the Zeeman splitting, we calculated the effective g value within the framework of this model. To the zeroth-order approximation, we neglected the effect of the extension of the exciton wave function in order to avoid using fitting parameters. Namely, the exciton is assumed to be localized at cationic ions. Wave functions of the excitons in PbI_2 corresponding to the four levels shown in Fig. 1 are described by the following equations:[11]

$$\phi^{1-}=-\sin\theta P_0 S|t_0\rangle - \frac{1}{\sqrt{2}}\cos\theta(P_{-1}S|t_{+1}\rangle - P_{+1}S|t_{-1}\rangle)\,, \tag{1}$$

$$\phi^{2-}=i\sin\theta P_0 S|s\rangle - \frac{i}{\sqrt{2}}\cos\theta(P_{-1}S|t_{+1}\rangle + P_{+1}S|t_{-1}\rangle)\,, \tag{2}$$

$$\phi^{3-}_{\pm}=-\sin\theta P_0 S|t_{\pm 1}\rangle - \frac{1}{\sqrt{2}}\cos\theta P_{\pm 1}S(-|s\rangle \pm |t_0\rangle)\,, \tag{3}$$

where the superscripts of the wave functions ϕ correspond to the character in the symmetry of D_{3d}. S and P_τ ($\tau=-1,0,+1$) stand for the $6s$ and $6p$ states of the Pb^{2+} ion, respectively. $|s\rangle$ and $|t_\kappa\rangle$ ($\kappa=-1,0,+1$) represent the singlet and triplet states of an electron-hole pair, respectively. The ϕ^{3-} states are doubly degenerate in zero field. The subscripts τ and κ stand for magnetic quantum numbers of the p state and z component of the total spin of an electron-hole pair, respectively. Therefore, ϕ^{2-} and $\phi^{3-}_{\pm}$ are z-like and x,y-like states, respectively, and ϕ^{1-} is a pure triplet state. θ is defined by the

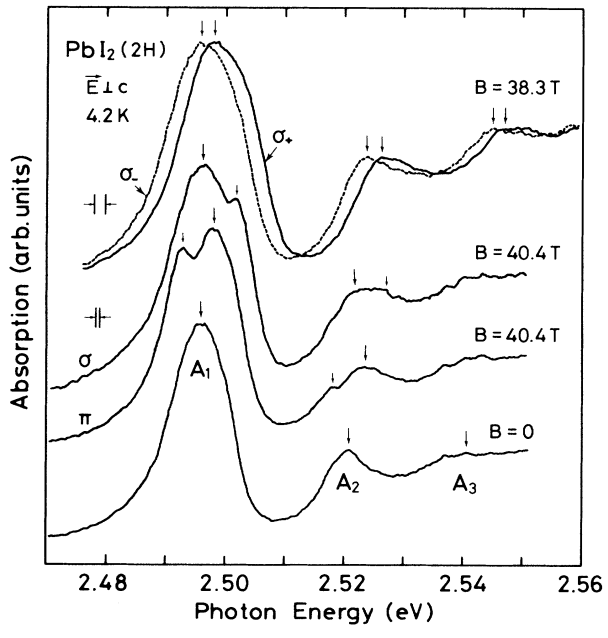

FIG. 4. Magnetoabsorption spectra of 2H-PbI_2 for (a) $\mathbf{E}\perp c\|\mathbf{B}$ and (b) $\mathbf{E}\perp c\perp\mathbf{B}$ at 4.2 K. Large down arrows display main absorption lines, which correspond to the absorption lines at $\mathbf{B}=0$, and small down arrows indicate magnetic-field-induced new lines.

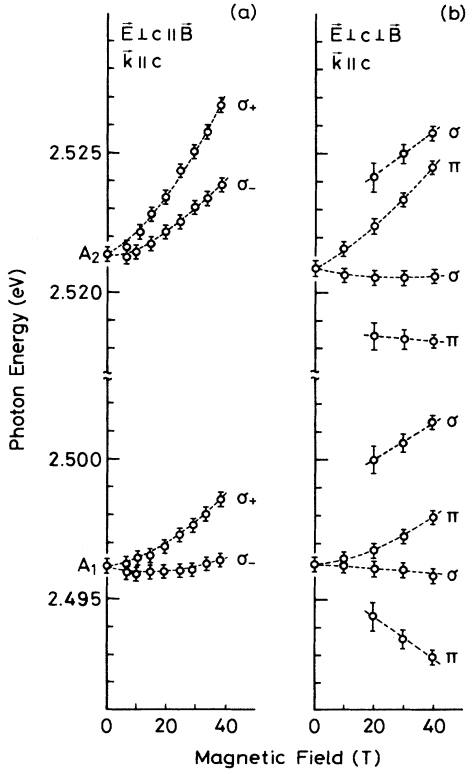

FIG. 5. Energy position of the ground-state absorption line as a function of magnetic field for (a) $\mathbf{E}\perp c\|\mathbf{B}$ and (b) $\mathbf{E}\perp c\perp\mathbf{B}$. The dashed lines are guides to the eye showing the energy change of the absorption lines.

spin orbit interaction parameter λ and the crystal-field splitting energy Δ as follows:

$$\tan 2\theta = \frac{2\sqrt{2}}{\lambda - 3\Delta}, \quad 0 \le \theta \le \frac{\pi}{2} . \tag{4}$$

The Zeeman term in the Hamiltonian is represented by

$$H = \frac{e}{2m_e}(\hat{l}_e + g_e \hat{s}_e)B - \frac{e}{2m_h}(\hat{l}_h + g_h \hat{s}_h)B , \tag{5}$$

where e is the charge of an electron, B is the applied magnetic field, and m_e and m_h are the mass of the electrons and holes, respectively. $\hat{l}_e$ and $\hat{l}_h$ are angular momentum operators, and $\hat{s}_e$ and $\hat{s}_h$ are spin momentum operators of electrons and holes, respectively. g_e and g_h are g factors of the electrons and holes, respectively.

On the basis of the present model, neglecting the effect of the extension of the exciton, let us adopt a mass and a g factor of free electrons in a vacuum in (5), namely we assume $m_e = m_h = m_0$ and $g_e = g_h = 2$, for simplicity. The effects from other ions or electrons and holes are treated as the uniaxial crystal-field energy Δ. For $\mathbf{B} \| z$ and $\mathbf{E} \| x,y$, the $\phi_{\pm}^{3-}$ are the observable states. From (3) and (5), the energy of the Γ_3^- state is obtained as

$$\mathcal{E}^3 = \mathcal{E}_3 \pm LB , \tag{6}$$

where $\mathcal{E}_3$ is the energy at $B = 0$ and

$$L = \mu_B(\sin^2\theta + 1) , \tag{7}$$

where μ_B is the Bohr magneton. Here, the effect of the spin-orbit split-off excitons is neglected, because the energy differences between the excitons and the band-edge exciton are much larger than the Zeeman energy. As shown in (6), the Zeeman splitting is a linear function of magnetic field in this configuration as was experimentally observed. Here, a diamagnetic term does not appear in this equation, because the extension of the exciton is neglected in the present model. The effective g value for the configuration of $\mathbf{E} \perp c \| \mathbf{B}$ is calculated as $g_\perp = 2L/\mu_B$. The spin-orbit interaction parameter λ and crystal-field splitting energy Δ have been estimated to be -0.95 and 0.75 eV, respectively.[7] These values render an effective g value as $g_\perp = 2.23$. The experimentally obtained effective g value of 0.89 (Ref. 5) is about one-half of the calculated value. It is considered that the extension of the actual exciton envelope function is larger than that in the atomic model, resulting in a smaller amplitude of the envelope function at the Pb^{2+} ion site. Hence, it is reasonable that the g value in real crystals is smaller than that in the atomic model corresponding to the smaller amplitude.

For the configuration of $\mathbf{E} \perp c \perp \mathbf{B}$, the symmetry reduction from the crystal symmetry of D_{3d} makes Γ_1^- and Γ_2^- states observable besides the Γ_3^- state in the presence of magnetic fields for π and σ polarizations, respectively.[11] Therefore, the new absorption lines observed with the configuration of $\mathbf{E} \perp c \perp \mathbf{B}$ are considered to be related to the ϕ^{1-} state for π and the ϕ^{2-} state for σ. For $\mathbf{B} \| x$, from (1)–(3) and (5) the energies of the diagonalized exciton states are

$$\mathcal{E}^1 = \tfrac{1}{2}\{(\mathcal{E}_1 + \mathcal{E}_3) \pm [(\mathcal{E}_1 - \mathcal{E}_3)^2 + 8M^2B^2]^{1/2}\} , \tag{8}$$

$$\mathcal{E}^2 = \tfrac{1}{2}\{(\mathcal{E}_2 + \mathcal{E}_3) \pm [(\mathcal{E}_2 - \mathcal{E}_3)^2 + 8N^2B^2]^{1/2}\} , \tag{9}$$

where $\mathcal{E}_1$, $\mathcal{E}_2$, and $\mathcal{E}_3$ are energies of Γ_1^-, Γ_2^-, and Γ_3^- states at $B = 0$, respectively, and M and N are defined by

$$M = \mu_B \left[-\sin\theta\cos\theta + \frac{1}{\sqrt{2}}(\sin^2\theta + 1) \right] , \tag{10}$$

$$N = i\mu_B \left[-\sin\theta\cos\theta - \frac{1}{\sqrt{2}}(\sin^2\theta + 1) \right] . \tag{11}$$

Thus, the nonlinear Zeeman splitting is expected as was actually observed in the experiment in this configuration. Here, the $\mathcal{E}^1$ is the allowed transition for π and $\mathcal{E}^2$ for σ. We can explain the qualitative feature of the ansiotropic Zeeman effect on the basis of the above-mentioned model.

Figure 6 shows energy shifts of the absorption lines as a function of the square of magnetic field, where the energy shift is defined as the average of the energy of the two absorption lines for σ_+ and σ_- polarizations of $\mathbf{E} \perp c \| \mathbf{B}$ or that for σ of $\mathbf{E} \perp c \perp \mathbf{B}$. From (6) and (9), the Zeeman terms cancel in these averages, and the resultant average should contain only the diamagnetic shift which was not taken into account in the calculation. It is obvious that the diamagnetic shift of the A_1 line is significant both for $\mathbf{E} \perp c \| \mathbf{B}$ and $\mathbf{E} \perp c \perp \mathbf{B}$ as shown in Fig. 6. The diamagnetic shift for $\mathbf{E} \perp c \perp \mathbf{B}$ is about one-half of that for $\mathbf{E} \perp c \| \mathbf{B}$. It is evident that the ground-state exciton is a more or less Wannier-type exciton as it shows B^2 dependence of the energy shift, and a hydrogenlike exciton model is still applicable to interpret the exciton. As for the A_2 line in particular for $\mathbf{E} \perp c \| \mathbf{B}$, sublinear energy shifts were observed against the square of the magnetic field. This energy dependence is explained in terms of an intermediate

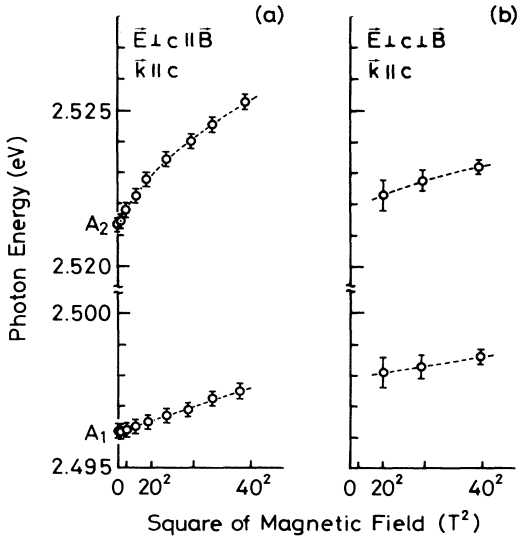

FIG. 6. Energy shifts of the absorption lines against the square of magnetic field for (a) $\mathbf{E} \perp c \| \mathbf{B}$ and (b) $\mathbf{E} \perp c \perp \mathbf{B}$. The dashed lines are guides to the eye showing the energy shift of the absorption lines.

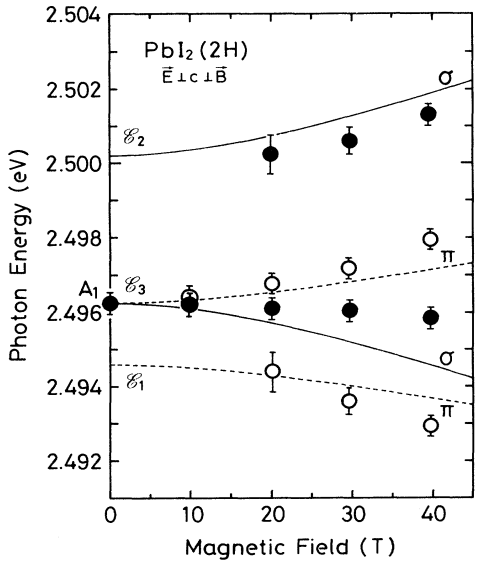

FIG. 7. Energy position of the ground-state absorption line for $\mathbf{E}\perp c\perp\mathbf{B}$. Open circles display experimental data for π and solid ones for σ. Broken lines are calculated curves for π and solid ones for σ.

magnetic-field effect and an exciton-phonon interaction.[5]

In order to make more quantitative comparison, we attempted a numerical calculation assuming the same values of parameters. Figure 7 shows the calculated curves of (8) and (9) with the configuration of $\mathbf{E}\perp c\perp\mathbf{B}$ together with the experimental results. Here, we assumed $\mathscr{E}_1=2.4946$ eV, $\mathscr{E}_2=2.5002$ eV, and $\mathscr{E}_3=2.4962$ eV. As for the g factor for $\mathbf{E}\perp c\|\mathbf{B}$ there is a discrepancy by a factor of 2 between the calculation and the experimental result; however, the calculated curve for $\mathbf{E}\perp c\perp\mathbf{B}$ is in relatively good agreement with the experimental result. On the other hand, diamagnetic shift for $\mathbf{E}\perp c\perp\mathbf{B}$ is about one-half of that for $\mathbf{E}\perp c\|\mathbf{B}$ as shown in Fig. 6. Therefore, it is considered that in the direction perpendicular to the layer, the exciton radius is even smaller, and the cationic exciton model is more applicable to explain the Zeeman splitting in this direction. The present results show that in the direction parallel to the layer the exciton in PbI_2 has a character as a Wannier-type exciton, whereas in the direction perpendicular to the layer, the exciton has a character more like a Frenkel-type exciton.

In conclusion, the magnetic-field effect of the exciton absorption lines in PbI_2 are measured up to 40 T with the configurations of $\mathbf{E}\perp c\|\mathbf{B}$ or $\mathbf{E}\perp c\perp\mathbf{B}$. An ansiotropic magnetic-field dependence of the spectra was observed. By comparing the experimental results and calculation based on the cationic exciton model, the following points were revealed. The observed Zeeman effect is qualitatively explained in terms of the cationic exciton model on which the uniaxial crystal-field related to the layered structure, spin-orbit interaction, and electron-hole coupling are taken into account. The deviation of the observed Zeeman effect from the calculation particularly for $\mathbf{E}\perp c\|\mathbf{B}$ is explained by the diamagnetic shift due to the extension of the exciton-wave function. The band-edge exciton in PbI_2 is a Wannier-type exciton, but has a cationic character at the same time. This character is a consequence of the small radius of the exciton in PbI_2. The uniaxial anisotropy due to the layered structure of PbI_2 gives rise to the zero-field splittings through the electron-hole exchange interaction and nonlinear Zeeman splitting for $\mathbf{E}\perp c\perp\mathbf{B}$.

*Present address: Research Center for Advanced Science and Technology, University of Tokyo, 4-6-1 Komaba, Meguro-ku, Tokyo 153, Japan.

[1]S. Nikitine and G. Perny, C. R. Acad. Sci. Paris **240**, 64 (1955).
[2]G. Harbeke and E. Tosatti, J. Phys. Chem. Solids **37**, 126 (1976).
[3]G. Baldini and S. Franchi, Phys. Rev. Lett. **26**, 503 (1971).
[4]L. C. Thanh, C. Depeursinge, F. Levy, and E. Mooser, J. Phys. Chem. Solids **36**, 69 (1875).
[5]Y. Nagamune, S. Takeyama, and N. Miura, Phys. Rev. B **40**, 8099 (1989).
[6]G. Harbeke and E. Tosatti, Phys. Rev. Lett. **28**, 1567 (1972).
[7]I. Ch. Schlüter and M. Schlüter, Phys. Rev. B **9**, 1652 (1974).
[8]G. Harbeke, F. Bassani, and E. Tosatti, in *Proceedings of the XIth International Conference on the Physics of Semiconductors* (PWN-Polish Scientific, Warsaw, 1972), p. 163.
[9]M. S. Skolnick and D. Bimberg, Phys. Rev. B **18**, 7080 (1978).
[10]J. Biellmann, V. Gubanov, B. Meyer, and C. Schwab, Phys. Status Solidi B **103**, 697 (1981).
[11]G. F. Koster, J. O. Dimmock, R. G. Wheeler, and H. Statz, *Properties of the Thirty Two Point Groups* (MIT Press, Cambridge, MA, 1963).
[12]Y. Nagamune, S. Takeyama, N. Miura, T. Minagawa, and A. Misu, Appl. Phys. Lett. **50**, 1337 (1987).
[13]S. Tarucha, H. Okamoto, Y. Iwasa, and N. Miura, Solid State Commun. **52**, 815 (1984).
[14]S. Takeyama, K. Watanabe, N. Miura, T. Komatsu, K. Koike, and Y. Kaifu, Phys. Rev. B **41**, 4512 (1990).